RSC Advances

PAPER

View Article Online
View Journal | View Issue

Cite this: *RSC Adv.*, 2022, **12**, 6007

Bio-AgNPs-based electrochemical nanosensors for the sensitive determination of 4-nitrophenol in tomato samples: the roles of natural plant extracts in physicochemical parameters and sensing performance†

Nguyen Le Nhat Trang, ‡[a] Dao Thi Nguyet Nga, ‡[a] Van-Tuan Hoang,*[a] Xuan-Dinh Ngo,[a] Pham Tuyet Nhung[a] and Anh-Tuan Le*[ab]

The present work reports efficient electrochemical nanosensors for the sensitive monitoring of 4-nitrophenol (4-NP) in tomato samples using various biosynthesized silver nanoparticles (bio-AgNPs). Three different bio-AgNP types were synthesized using natural plant extracts, including green tea (GT) leaf, grapefruit peel (GP), and mangosteen peel (MP), aiming to investigate their effects on the formation of bio-AgNPs, as well as the analytical performance of 4-NP. Based on the obtained results, it was found that the phytochemical content in various plant extracts directly influenced the physicochemical parameters of the created bio-AgNPs, such as particle size, crystallinity, and distribution. More importantly, these parameters have decisive effects on the electrocatalytic activity, conductivity, and electrochemical sensing performance of electrodes modified with them for 4-NP detection. Among the three bio-AgNPs evaluated, the GT-AgNPs (using green tea leaf extract) with uniform shape, small size without aggregation, and high crystallinity showed the best analytical performance for 4-NP determination. The electrode-modified GT-AgNPs exhibited a good 4-NP analytical performance with an electrochemical sensitivity of 1.25 μA μM^{-1} cm^{-2} and a detection limit of 0.43 μM in the detection range from 0.5 to 50 μM. The practical applicability of the sensor was also studied in tomato samples, promising satisfactory results toward 4-NP detection in other real samples.

Received 20th December 2021
Accepted 7th February 2022

DOI: 10.1039/d1ra09202b

rsc.li/rsc-advances

1. Introduction

Nowadays, the pesticide residues on crops are a major threat to human health and the surrounding environment, leading to a variety of deteriorative consequences. Among them, 4-nitrophenol (4-NP) detection is particularly attempted due to its toxicity and hazard.[1] 4-NP can remain in irrigation water for a long time, causing undesirable effects to humans, animals, and crops. Since the 1980s, 4-NP has been classified as a priority hazardous pollutant by the US Environmental Protection Agency (US EPA). Accordingly, the maximum permissible concentration limit of 4-NP should be less than 20 μg L^{-1}.[2,3] In fact, the 4-NP treatment and removal are quite difficult because of its high stability and solubility.[1] Therefore, it is necessary to develop an analytical tool for the effective and quick detection of 4-NP in contaminated samples.

There are various analytical techniques to determine 4-NP residues, including capillary electrophoresis,[4] fluorescence,[5] flow-injection analysis,[6] high-performance liquid chromatography (HPLC),[7] and enzyme-linked immunosorbent assay (ELISA).[8] Although these techniques have high specificity and selectivity, they require expensive instruments and reagents, multi-step analytical techniques, and consume organic solvents. Thus, the development of a simple analytical technique, with characteristics of low cost, quick detection, and a simple system for 4-NP detection is considered a necessary and important strategy. The electrochemical sensor technique has been proven to be a potential solution for 4-NP detection because of its advantages such as good sensitivity, fast response, simple sample pre-treatment, low cost, easy operation, and onsite detection.[9–11] In recent years, the modification of the working electrode surface has been reported as effectively capable of enhancing the sensitivity, selectivity, and stability of sensors for 4-NP detection.[9,10,12] For example, Ikhsan *et al.*[9] used reduced graphene oxide-silver (rGO-Ag) nanocomposites to modify glassy carbon electrodes (GCE) for the detection of 4-NP.

[a]*Phenikaa University Nano Institute (PHENA), PHENIKAA University, Hanoi 12116, Vietnam. E-mail: tuan.hoangvan@phenikaa-uni.edu.vn*

[b]*Faculty of Materials Science and Engineering (MSE), PHENIKAA University, Hanoi 12116, Vietnam. E-mail: tuan.leanh@phenikaa-uni.edu.vn*

† Electronic supplementary information (ESI) available. See DOI: 10.1039/d1ra09202b

‡ N. L. N. Trang and D. T. N. Nga contributed equally to this work.

The results showed that the rGO-Ag-modified electrode provided a low detection limit of 1.2 nM. Many other nanomaterials, including silver nanowire-polyaniline,[12] GO film,[10] Mg(Ni)FeO,[11] and bio-AgNPs[13] have also been used to modify electrode surfaces, aiming to enhance the 4-NP sensing performance with wider linear ranges and lower limits of detection (LOD). In our previous work, a screen-printed electrode (SPE) modified with bio-AgNPs synthesized from green tea leaf (*Camellia sinensis*) extract was used for the first time as a promising electrode toward 4-NP sensing.[14] For more detailed assessments on the promising potential of bio-AgNPs in modifying the electrode surface, this study has systematically evaluated the bio-Ag formation from different natural extracts and their effects on some parameters such as electrical resistance, amperage, and electrochemical stabilization in the electrochemical sensor performance. The electrochemical properties of the bio-AgNPs-modified SPE were significantly enhanced in comparison with bare SPE and pure AgNPs-SPE. The presence of biomolecules on the bio-AgNPs surface facilitated the effective attachment of AgNPs on the carbon surface of the screen-printed carbon electrode (SPE) through the formation of strong C–O coordinate bonds between the O atoms of oxygen functional groups and the C atom of SPE. The utilization of bio-AgNPs in electrochemical nanosensors in detecting various pollutants is the preferred trend because of its low toxicity and good biocompatibility.[15] Nonetheless, some critical problems need to be further understood regarding the effects of the morphology, size distribution, and crystallinity of bio-AgNPs synthesized from the various bio-reducing agents on the selectivity and sensitivity of the sensor.[16,17]

We have synthesized bio-AgNPs from various natural plant extracts, including green tea leaves (*Camellia sinensis*), mangosteen peel (*Garcinia mangostana*), and grapefruit peel (*Citrus paradisi*) by a simple electrochemical method. Herein, we aim to gain insight into the influences of the phytochemical components and content in each plant extract on the physicochemical parameters of the created bio-AgNPs such as particle size, crystallinity, and distribution. The impacts of these parameters on the electrochemical sensor performance toward 4-NP detection have been investigated in detail, promising the development of an effective tool for monitoring 4-NP residues in crops.

2. Experimental procedures

2.1. Chemicals

Two bulk silver bars (99.999% purity) with dimensions of 150 mm × 10 mm × 0.5 mm ($L \times W \times T$) were used as electrodes and were purchased from a domestic jewelry company in Hanoi, Vietnam. 4-Nitrophenol (4-NP, 98%), nitric acid (HNO_3, 63%), iron(III) nitrate ($Fe(NO_3)_3$, 99%), copper(II) sulfate ($CuSO_4$,99%), zinc nitrate ($Zn(NO_3)_2$, 99%), nickel(II) nitrate ($Ni(NO_3)_2$, 99%), potassium chloride (KCl, 99%), ascorbic acid ($C_6H_8O_6$, 99%), urea (CH_4N_2O, 99%), thiram ($C_6H_{12}N_2S_4$,99%), amoxicillin ($C_{16}H_{19}N_3O_5S$, 99%), and D-glucose ($C_6H_{12}O_6$, 99%) were purchased from Shanghai Chemical Reagent. The PBS buffer solution (0.1 M, pH 7.2) was prepared by using NaCl, KCl, $Na_2HPO_4 \cdot 12H_2O$, and KH_2PO_4 (>99%, Merck KGaA, Germany). The pH of the PBS buffer was adjusted using H_3PO_4 (0.1 M) and NaOH (2 M). All chemicals were used as received without any further purification. Carbon screen-printed electrodes (SPEs-DS110) were purchased from DS Dropsens, Spain.

2.2. Preparation of the bio-AgNPs-modified SPEs

Bio-AgNPs were synthesized from natural plant extracts by a modified electrochemical method.[14] In brief, the process for the synthesis of bio-AgNPs was based on a two-electrode setup system in combination with the controlled addition of various natural plant extracts. The two silver bars as electrodes were mechanically polished and washed with distilled water to eliminate oxides on the surface. They were connected to the DC voltage source in parallel in the 250 mL glass beaker placed on the magnetic stirrer. The distance between the two electrodes was about 3 cm, and bi-distilled water was poured for 6 cm of silver electrodes. Then, 15 mL of each plant extract, namely, green tea leaves (bio-GT), mangosteen peel (bio-MP), and grapefruit peel (bio-GP), were added and stirred for 10 minutes, respectively. The silver bars were supplied with a DC voltage of 12 V for 45 minutes under magnetic stirring at room temperature.

To prepare bio-AgNPs-modified SPE electrodes, the bio-AgNPs solutions with various volumes from 4 to 14 μL were directly dropped onto the working electrode surface and dried at room temperature.

2.3. Spiked tomato sample preparation

Tomatoes were purchased from a local supermarket and washed with deionized water, and then naturally dried before extraction. Next, 5 g of tomato were mixed with 10 mL PBS (0.1 M) by a vortex mixer. The mixture was ultrasonicated for 30 min, then the resulting mixture was centrifuged for 10 min at 10 000 rpm, and the clear liquid phase was collected and 4-NP with different concentrations was added (5, 10, and 20 μM).

2.4. Characterization techniques

The crystalline structure of the bio-AgNPs samples was analyzed by a Bruker D5005 X-ray diffractometer (using Cu Kα radiation, $\lambda = 0.154056$ nm) under a voltage of 40 kV and a current of 30 mA. The bio-AgNPs formation was confirmed by ultraviolet-visible (UV-vis) spectrophotometry (HP 8453 spectrophotometer). All electrochemical measurements were conducted on an electrochemical workstation (Palmsens4, PS Trace, PalmSens, The Netherlands) at room temperature.

2.5. Electrochemical measurements

Cyclic voltammetry (CV) measurements were carried out in 0.1 M KCl containing 5 mM $[Fe(CN)_6]^{3-/4-}$ at a scan rate of 50 mV s^{-1} with a potential range from −0.3 V to 0.6 V. Electrochemical impedance spectroscopy (EIS) was recorded in the frequency range of 0.01–50 kHz by applying an AC voltage with 10 mV amplitude in 0.1 M KCl containing 5 mM $[Fe(CN)_6]^{3-/4-}$. The electrochemical performance of 4-NP on the modified SPE

was investigated using CV and differential pulse voltammetry (DPV) measurements in aqueous phosphate buffer electrolyte solution (PBS, 0.1 M). The CV was obtained at a scan rate of 60 mV s^{-1} in the potential range from −1 to 0 V, $T_{equilibrium}$ = 120 s. The DPV measurements were completed as follows: scan rate of 6 mV s^{-1}, $T_{equilibrium}$ = 120 s, E_{pluse} = 0.075 V, T_{pulse} = 0.2 s in the potential range of −0.2 to −0.7 V.

3. Results and discussion

3.1. Characterization of bio-AgNPs

Three different solutions of bio-AgNPs were synthesized by a simple electrochemical method using three natural plant extracts including green tea leaves (GT-AgNPs), mangosteen peel (MP-AgNPs), and grapefruit peel (GP-AgNPs) to investigate their electrochemical sensing performances toward 4-NP detection. UV-vis spectrometry and SEM were utilized to confirm the formation of bio-AgNPs and investigate their structural features. Fig. 1(a–c) shows the UV-vis spectra of the as-synthesized bio-AgNPs samples and their colors. After the electrochemical process, the color of the extracted mixture changed to yellowish-brown, demonstrating the formation of AgNPs.[18,19] The formation of the AgNPs was also further confirmed *via* recording the characteristic surface plasmon resonance (SPR) absorption band at around 430–440 nm in the UV-vis region. Note that the absorption peak was found at 440 nm for both GT-AgNPs and GP-AgNPs, while that of MP-AgNPs was about 430 nm. Fig. 1(d–f) shows SEM images of the as-synthesized bio-AgNPs samples. All the bio-AgNPs samples had a uniform spherical shape with the size of about 10–25 nm. More importantly, when considering the dispersibility of bio-AgNPs, GT-AgNPs exhibited homogeneous distribution without the aggregation phenomenon; in contrast, for MP-AgNPs and GP-AgNPs samples, the created AgNPs tended to aggregate, leading to the formation of larger clusters (Fig. 1(e and f)). This phenomenon was proposed to be due to the differences in the ingredients and contents of the valuable beneficial phytochemicals in each extract type. Polyphenolic compounds have been considered among the major and most important reducing agents in plant extracts, which helps in promoting the bio-reduction of Ag^{+} to Ag^{0}. However, the components and content of these polyphenolic compounds in each plant extract are different, as described in some previous reports. In the GT extract, polyphenols (catechins, tannins) and alkaloids have been considered as the major phytochemical components that act as reducing and stabilizing agents for the bio-AgNPs.[20] These useful polyphenolic substances were also found in the GP and MP extracts.[21,22] However, it should be noted that in addition to such compounds, a large amount of other bioactive substances, such as xanthones and flavonoids were recorded in the MP extract, while, for the GP extract, limonene was the main component that occupied up to 60–95% w/w.[23] It is likely that these directly impacted the efficiency of the reduction process and the stability of the formed bio-AgNPs. Indeed, with a high content of polyphenolic compounds in the GT extract, the reduction process of Ag^{+} ions occurred more easily than that in the MP and GP extracts, and the stability of the bio-AgNPs was also improved due to these polar polyphenolic layers. In contrast, for the GP and MP extracts, the presence of low-polar and/or nonpolar organic compounds around the formed bio-AgNPs, such as xanthones and limonenes could cause the unwanted aggregation phenomenon in water.

The bio-AgNPs formation and particle size were further determined by TEM images. Fig. S1† shows TEM images of bio-AgNPs samples synthesized from three different extracts. The results showed that the nanoparticles had a spherical shape with an average size of 15–50 nm. The GT-AgNPs were uniformly dispersed by polyphenols, and the MP-AgNPs and GP-AgNPs showed the phenomenon of agglomeration.

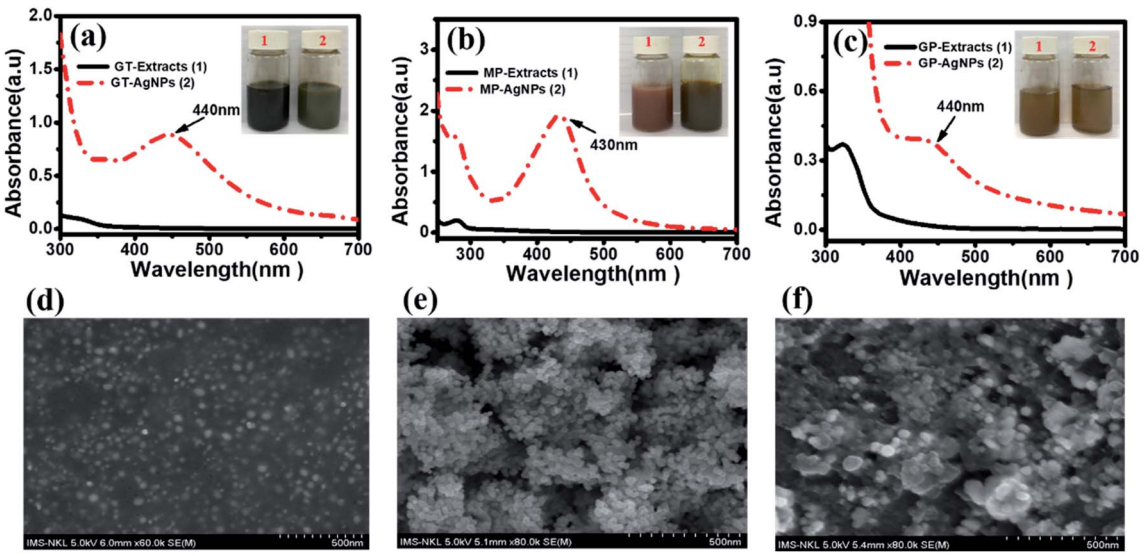

Fig. 1 UV-vis spectra of bio-AgNPs synthesized using different extracts: (a) GT-AgNPs; (b) MP-AgNPs; and (c) GP-AgNPs. Inset pictures show the glass vitals of extracts and bio-AgNPs solutions, respectively. (d, e and f) SEM images of GT-AgNPs, MP-AgNPs, and GP-AgNPs, respectively.

The presence of polyphenols from natural extracts on the nanoparticle surface was confirmed by Fourier-transform infrared (FTIR) spectroscopy (Fig. S2†). All three bio-AgNPs samples showed wide banding and high intensity at 3420 cm^{-1}, related to the O–H stretching oscillations assigned to the –OH groups from polyphenols in green tea extracts such as catechins.[24] The peak at 1630 cm^{-1} was associated with prolonged C=O oscillations of the conjugate bound to ketones, quinones, carboxylic acids and esters.[19] At 1392 cm^{-1}, there was the C–N stretching oscillation of aromatic amines, which was found only in GT-AgNPs samples, indicating the presence of EGCG in the water-soluble green tea extract. The band at 1044 cm^{-1} was found to be associated with the C–O–C stretching oscillation.[25] These results agreed with previous reports[18,26,27] and demonstrated the presence of polyphenols in the natural extract as surface protectants for bio-Ag seeds.

To analyze in detail the crystalline structural features of the three bio-AgNPs samples, XRD measurements were also performed. The obtained results are presented in Fig. 2. For all three bio-AgNPs solutions, the XRD patterns exhibited four diffraction peaks at 38.1°, 44.3°, 64.4°, and 77.5° corresponding to the (111), (200), (220), and (311) fcc crystal planes of bulk Ag (JCPDS PDF 04-0783), respectively. The average crystalline sizes were approximately calculated as 11, 13, and 19 nm by the Debye–Scherrer equation for GT-AgNPs, MP-AgNPs, and GP-AgNPs, respectively. Clearly, *via* the study on the characterization of bio-AgNPs in both three extract solutions, GT-AgNPs showed more outstanding features in not only size and crystallinity but also their distribution. Thus, GT-AgNPs was expected to be a key candidate having high potential to enhance electrocatalytic activity, as well as electron conductivity in the sensing electrode. This structural property–performance relationship was investigated and is discussed in more detail in the subsequent sections.

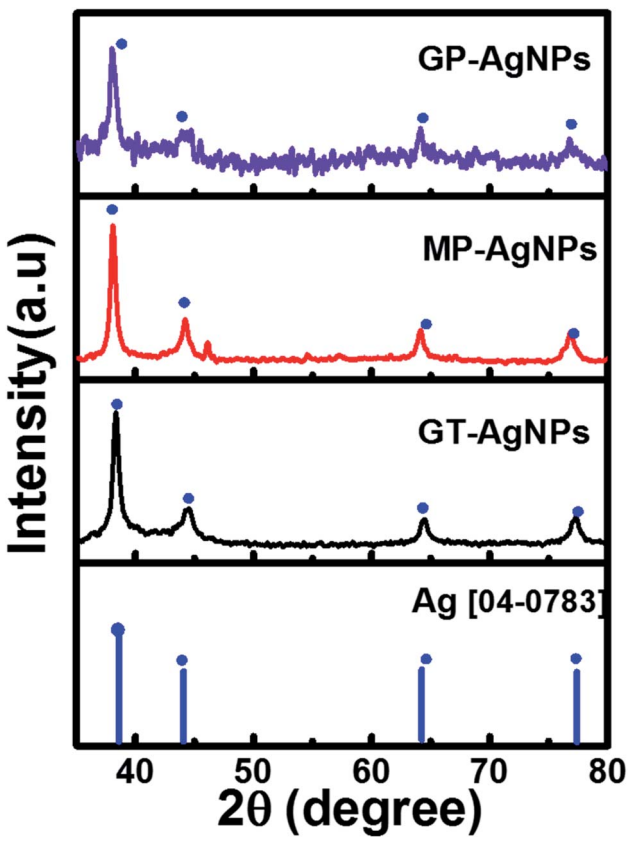

Fig. 2 XRD patterns of GT-AgNPs, MP-AgNPs, and GP-AgNPs, respectively.

3.2. Electrochemical investigations

3.2.1. Electrode characterization. In the initial step of the electrochemical performance analysis, the electrochemical characterizations of the bio-AgNPs-modified electrodes were investigated using cyclic voltammetry measurements (CV) in 0.1 M KCl containing 5 mM $[Fe(CN)_6]^{3-/4-}$ at a scan rate of a 50 mV s^{-1}. As shown in Fig. 3a, a pair of reversible redox peaks arising from the reversible electronic transfer of Fe^{2+} into Fe^{3+} and *vice versa* was observed at all three modified electrodes. However, there were obvious differences in the recorded peak current intensities for each modified electrode.[28,29] These differences could be ascribed to the changes in conductibility, electron transfer capability, as well as crystalline structural features of each bio-AgNPs type. The GT-AgNPs (102 μA) exhibited the largest current intensity (I_{pc}), compared with MP-AgNPs (56 μA) and GP-AgNPs (32 μA), as presented in Table 1.

Electrochemical impedance spectroscopy (EIS) has been considered an effective method for investigating the charge transfer capability of modified electrodes. Fig. 3(b) shows the Nyquist plots of GT-AgNPs/SPE, MP-AgNPs/SPE, and GP-AgNPs/SPE in 0.1 M KCl containing 5 mM $[Fe(CN)_6]^{3-/4-}$ in the frequency range of 50 kHz–0.01 Hz with 10 mV amplitude of the AC voltage. Herein, the radius of the semicircle represents the electron transfer resistance (R_{ct}), which was detected to be 661.6, 318, 638, and 1596 Ω for SPE, GT-AgNPs/SPE, MP-AgNPs/SPE, and GP-AgNPs/SPE, respectively. As a result, GT-AgNPs/SPE showed the lowest R_{ct} value as compared to the other modified electrodes, even bare SPE. Furthermore, the electroactive surface area (EASA) of the modified electrodes was determined *via* the CV technique under the scan rate in the range from 10 to 60 mV s^{-1}, as shown in Fig. 4(a–c). The corresponding linear plots of reduction peak current intensity against the square root of the scan rate are presented in Fig. 4(d–f). The EASA of these electrodes were calculated according to the Randles–Sevcik equation as follows (25 °C):

$$I_p = 2.69 \times 105An^{3/2}D^{1/2}Cv^{1/2} \quad (1)$$

where I_p presents the cathodic and anodic peak current, n is the number of electrons transferred, D is the diffusion coefficient of $[Fe(CN)_6]^{3-/4-}$, A is EASA, v is the potential scan rate, and C is the concentration of $[Fe(CN)_6]^{3-/4-}$. Herein, EASA was estimated from the graphs of the cathodic peak current along with $n = 1$, $D = 6.5 \times 10^{-6}$ cm s^{-1}, $C = 5$ mM, $v = 0.05$ V s^{-1}, as listed in Table 1. Accordingly, the estimated EASA value increased in the order GP-AgNPs (0.125 cm^2) < MP-AgNPs (0.262 cm^2) < GT-AgNPs (0.373 cm^2). From the obtained results for current response intensity, electron transfer resistance (R_{ct}), and EASA

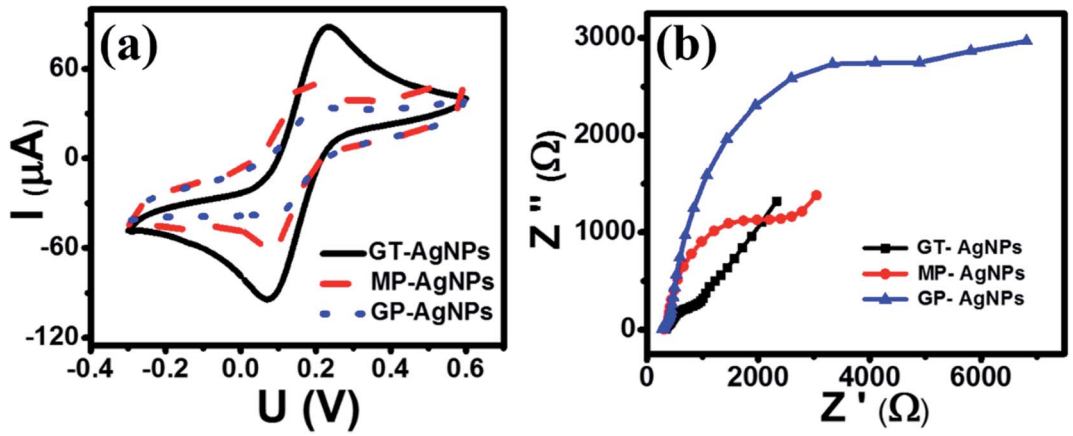

Fig. 3 (a) CV profiles of various modified electrodes at the scan rate of 50 mV s^{-1} in 0.1 M KCl containing 5 mM $[Fe(CN)_6]^{3-/4-}$; (b) EIS profiles of various modified electrodes.

Table 1 The current response of modified electrodes and their calculated EASA according to the Randles–Sevcik equation in 0.1 M KCl containing 5 mM $[Fe(CN)_6]^{3-/4-}$

Sample	I_{pc} (μM)	EASA (cm^2)
GT-AgNPs	102.18	0.373
MP-AgNPs	57.31	0.262
GP-AgNPs	31.65	0.125

value, it can be seen that as expected, the small and uniform size with high crystallinity, as well as the homogenous distribution of GT-AgNPs, helped them achieve fast electron transfer ability and large active surface area, which are promising for the effective reduction of 4-NP.

3.2.2. Electrochemical performance of 4-NP on the modified electrodes. To evaluate the electrochemical response of various bio-AgNPs toward 4-NP, the CV responses of the unmodified SPE and SPE modified with GT-AgNPs, MP-AgNPs, and GP-AgNPs toward 50 μM 4-NP were recorded. Fig. 5(a) shows the CV curves of all four electrodes in 0.1 M PBS (pH 5) containing 50 μM 4-NP. It can be seen that the sharp reduction peaks appeared at −0.81, −0.84, and −0.86 V for GP-AgNPs, MP-AgNPs, and GT-AgNPs, respectively. These reduction peaks could be assigned to the reduction of 4-NP involving the formation of 4-hydroxyaminophenol,[30] consistent with some previous reports for the reduction of 4-NP.[12,14,30] However, the current responses of these reduction peaks were remarkably different. Fig. 5(b) shows the bar chart diagram of the reduction

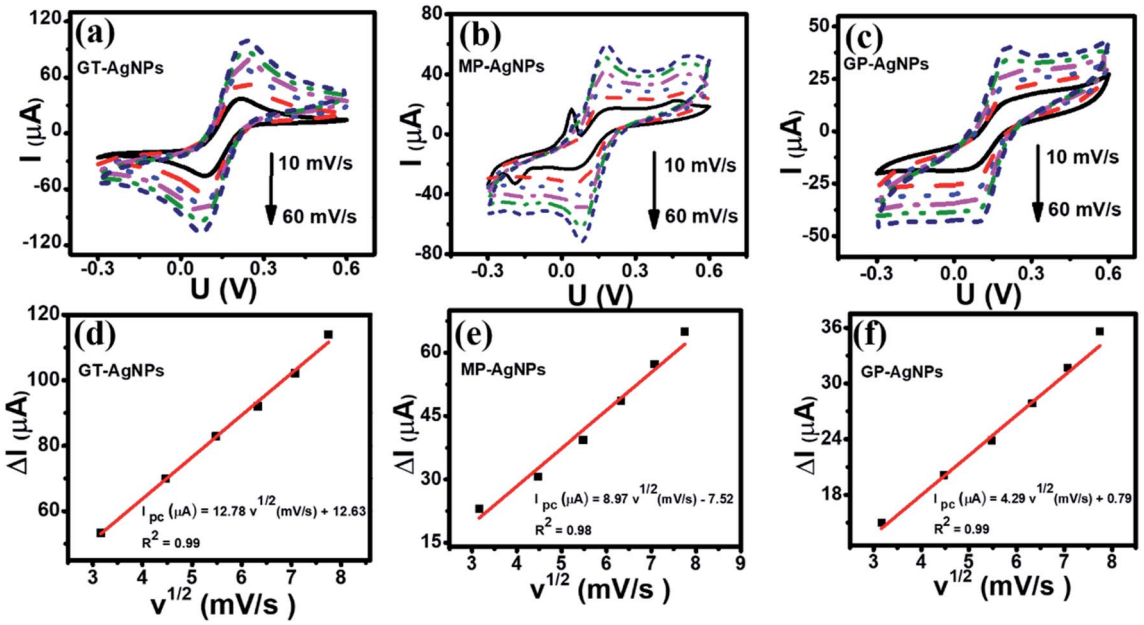

Fig. 4 (a–c): CV profiles of modified electrodes at various scan rates (10–60 mV s^{-1}); (d–f): the corresponding linear plots of reduction peak current response and sqrt of the scan rate. All experiments were performed in 0.1 M KCl containing 5 mM $[Fe(CN)_6]^{3-/4-}$.

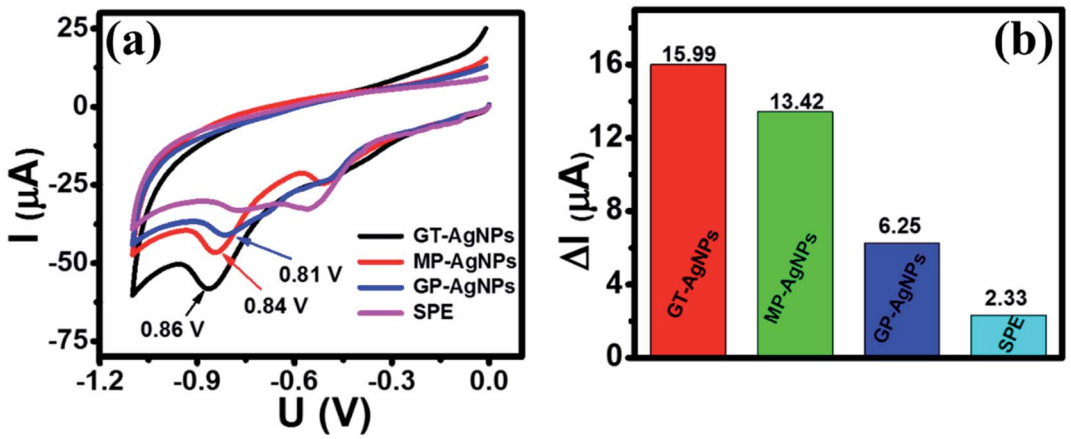

Fig. 5 (a) CV curves recorded for the unmodified SPE, GT-AgNPs, MP-AgNPs, and GP-AgNPs using 0.1 M PBS (pH 5) containing 50 μM 4-NP; (b) bar chart diagram of the irreversible reduction peak current responses for 4-NP over modified SPEs. Scan rate 50 mV s^{-1}.

peak current responses for 4-NP for all electrodes. Compared with the unmodified-SPE, all the modified SPE showed increases in the reduction peak current, suggesting that bio-AgNPs significantly improved electrochemical activity for the reduction of 4-NP. It is no surprise that GT-AgNPs afforded the highest cathodic peak current of about 15.99 μA, which was about 1.2 times that of MP-AgNPs (13.42 μA), 2.5 times that of GP-AgNPs (6.25 μA), and 6.8 times that of the bare SPE. The differences in the reduction peak potential of 4-NP were recorded for GP-AgNPs and MP-AgNPs. The reduction peak potentials of 4-NP on GP-AgNPs and MP-AgNPs were slightly shifted toward the more positive direction as compared with GT-AgNPs. This phenomenon could be due to the difference in pH value on the electrode surface after modification, arising from the pH differences of various bio-AgNPs solutions. The pH values of the three bio-AgNPs solutions were determined to be about 6.2, 5.4, and 5.1 for GT-AgNPs, MP-AgNPs, and GP-AgNPs, respectively. It is clear that the size, crystallinity, and distribution of bio-AgNPs strongly depend on the components and contents of the phytochemicals in each extract type, and are important factors affecting the electrochemical response toward 4-NP detection. Therefore, the understanding and selection of suitable plant extracts for synthesizing AgNPs for the various application aims are very important and necessary. To gain insight, the modified electrodes were further investigated in detail to determine the electrochemical properties for the sensing of 4-NP.

3.2.2.1 Optimization of the 4-NP determination conditions. To optimize the loading volume of AgNPs solution on the SPEs, the electrochemical responses of MP-AgNPs/SPEs with the various MP-AgNPs solution volumes from 4 to 14 μL were investigated by the DPV technique for 50 μM 4-NP in the 0.1 M PBS at a scan rate of 6 mV s^{-1} (see Fig. S3†). The reduction peak current of 4-NP increased significantly with the increase of the modifier volume up to 12 μL. The peak current gradually decreased with further increasing the modifier amount. The high increase of the MP-AgNPs volume caused the increase in the thickness of the modifier layer on the electrode surface, which not only hindered the electron transfer within the electrode and the access of the electrolyte to the electrode surface but also led to the easy peeling and breaking of the working electrode during operation.[31] Thus, the optimized value of MP-AgNPs volume was proposed to be 12 μL for the next electrochemical measurements.

The influence of pH on the current and potential of the reduction peak was investigated by using the DPV technique. DPV curves of MP-AgNPs/SPE for 10 μM CAP in the 0.1 M PBS in the pH range from 3 to 11 are shown in Fig. S4.† The peak current response gradually increased on varying the pH from 3 to 5. This proposes that the reduction of 4-NP is a pH-dependent process and the hydrogen ions interrupt the 4-NP redox reactions.[32] However, beyond the pH value of 5, a further increase in the pH led to a decrease in the peak current response. Therefore, PBS (pH 5) was the best condition for obtaining the highest current response for the detection of 4-NP.

For the effect of accumulation time, the MP-AgNPs-modified SPE was investigated in the accumulation time range from 30 to 150 s to determine the optimum time as shown in Fig. S5.† The peak current intensity (I_p) increased with increasing accumulation time and reached a maximum at 120 s. Thus, the suitable accumulation time was chosen as about 120 s for the next electrochemical experiments. For insight into the relationship between the scan rate and the current response and/or peak potential, a kinetics study through CV measurements was conducted. Fig. S6(a)† illustrates the influence of various scan rates (10–50 mV s^{-1}) on the electrochemical behaviours of 4-NP in 0.1 M PBS (pH 5) containing 40 μM 4-NP. An increase in the cathodic peak currents was recorded with an increase in the scan rate for the electrode studied. Fig. S6(b)† shows the calibration plot between the irreversible reduction peak current of 4-NP and scan rate. The current response showed a linear relationship with the scan rate, corresponding to linear regression equations: I_p (μA) = 0.077v (mV s^{-1}) + 1.58 (R^2 = 0.99). Accordingly, the redox process of 4-NP at bio-AgNPs/SPE was the typical surface adsorption-controlled process.

3.2.2.2 Calibration curve. DPV is an efficient measurement that can be detected and quantified in very small amounts of

targeted analytes. Thus, it was utilized herein to evaluate the 4-NP analytical performance on the various bio-AgNPs-based electrochemical sensors. Fig. 6 shows the DPV curves of 4-NP with various concentrations on the electrodes modified with GT-AgNPs (a), MP-AgNPs (b) and GP-AgNPs (c) in 0.1 M PBS (pH 5) under the above optimal conditions, and the respective calibration plots of peak current intensities against various concentrations of 4-NP. The reduction peak current increased with an increase in the concentration of 4-NP for all the modified electrodes. The calibration plots were constructed for each modified electrode with the coefficient of correlation R^2 being more than 0.99, as shown in Fig. 6(d–f). The regression equations were as follows: I_p (μA) = 0.173C (μM) + 0.487 (R^2 = 0.99) for GT-AgNPs; I_p (μA) = 0.142C (μM) + 0.03 (R^2 = 0.99) for MP-AgNPs; and I_p (μA) = 0.091C (μM) − 0.32 (R^2 = 0.99) for GP-AgNPs. Furthermore, it was observed that the reduction potential slightly shifted to the more negative direction along with the increased 4-NP concentration, which is attributed to the involvement of protons and the change in the pH value around the electrode interface.[17]

In comparison with two other modified electrodes, the GT-AgNPs exhibited the highest electrochemical sensitivity up to 1.25 μA μM^{-1} cm^{-2} along with the lowest detection limit of 4-NP of about 0.42 μM in the wider linear range from 0.5 to 50 μM. The electrochemical sensitivity of MP-AgNPs was calculated to be 1.04 μA μM^{-1} cm^{-2} with a detection limit of about 0.63 μM in the concentration linear range from 1 to 50 μM. Besides, the lowest electrochemical sensitivity about 0.35 μA μM^{-1} cm^{-2} was observed on the GP-AgNPs with a detection limit of 0.82 μM in the linear range of 1–50 μM. In short, GT-AgNPs achieved a higher sensitivity with lower LOD in a wider linear range for the determination of 4-NP as compared to MP-AgNPs and GP-AgNPs. Based on the obtained results from the material characterizations and electrochemical properties of three bio-AgNPs as well as the electrochemical performance of 4-NP, the 4-NP sensing performance of the electrodes modified with bio-AgNPs considerably depends upon the size, crystallinity, and distribution of bio-AgNPs, which are directly affected by the plant extract components.

The oxidation–reduction pathway of 4-NP in the presence of bio-AgNPs was displayed by two processes (Fig. 7): (1) first, the 4-NP tends to lose four electrons and four protons ($4H^+$, $4e^-$) to form 4-hydroxylaminophenol and this is an irreversible process. (2) 4-NP was reverted from the reversible oxidation–reduction reaction of 4-hydroxylaminophenol involving the two electrons and two protons ($2H^+$, $2e^-$).[8] Thus, the redox pair (E_{pa} = 0.23 V and E_{pc} = 0.07 V) can be assigned as 4-hydroxyaminophenol and 4-nitrosophenol, respectively.

3.2.2.3 Repeatability, stability, reproducibility and selectivity studies of the portable electrochemical sensing system. Under the same conditions, the repeatability of the modified electrodes was evaluated by recording the current response in the presence of 50 μM 4-NP for 10 successive times on the same electrodes. Fig. S7(a–c)† shows the reduction current of 4-NP for the GT-AgNPs, MP-AgNPs, and GP-AgNPs. The obtained results demonstrated that these sensors possessed good repeatability with low relative standard deviation (RSD) values of 1.25%, 1.4%, and 1.48% for GT-AgNPs, MP-AgNPs, and GP-AgNPs, respectively. The selectivities of the bio-AgNPs-modified electrodes were analyzed by the DPV technique in the presence of various interfering compounds and ions. The tested results showed that the presence of 200 μM of K^+, Zn^{2+}, Ni^{2+}, Fe^{2+}, Cu^{2+}, Cl^-, NO_3^-, and SO_4^{2-} ions and 200 μM of various compounds, such as D-glucose, ascorbic acid, urea, thiram, and amoxicillin

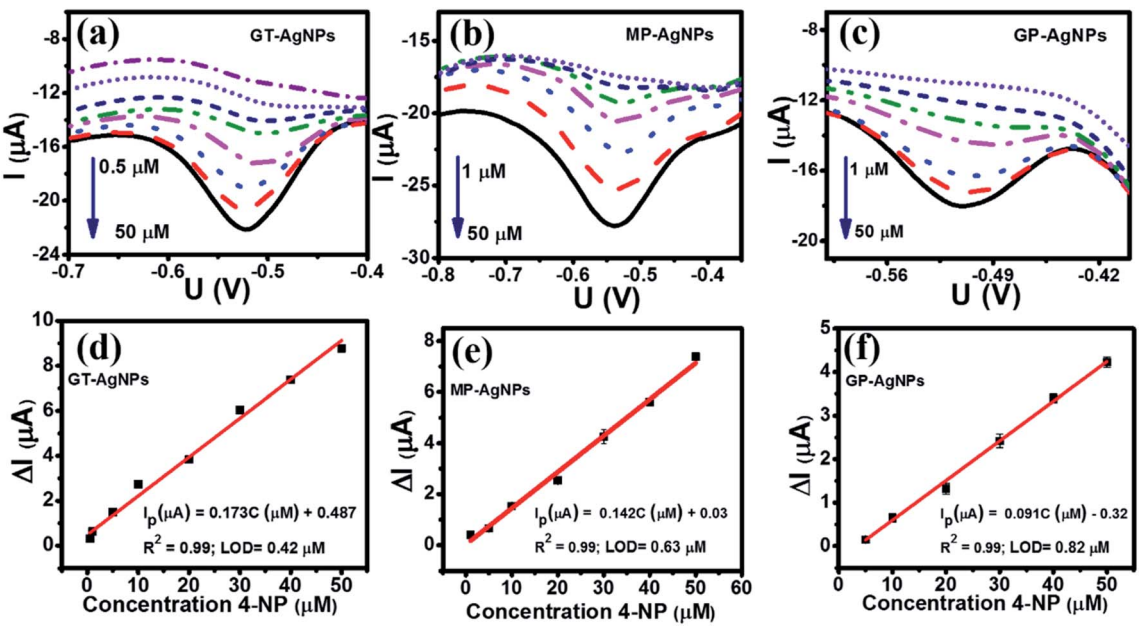

Fig. 6 DPV curves at various concentrations of 4-NP in 0.1 M PBS (pH 5) with a scan rate of 50 mV s^{-1} for GT-AgNPs (a), MP-AgNPs (b), and GP-AgNPs (c); the corresponding calibration plots of peak current intensity *vs.* various concentrations of 4-NP (d–f) with error bars.

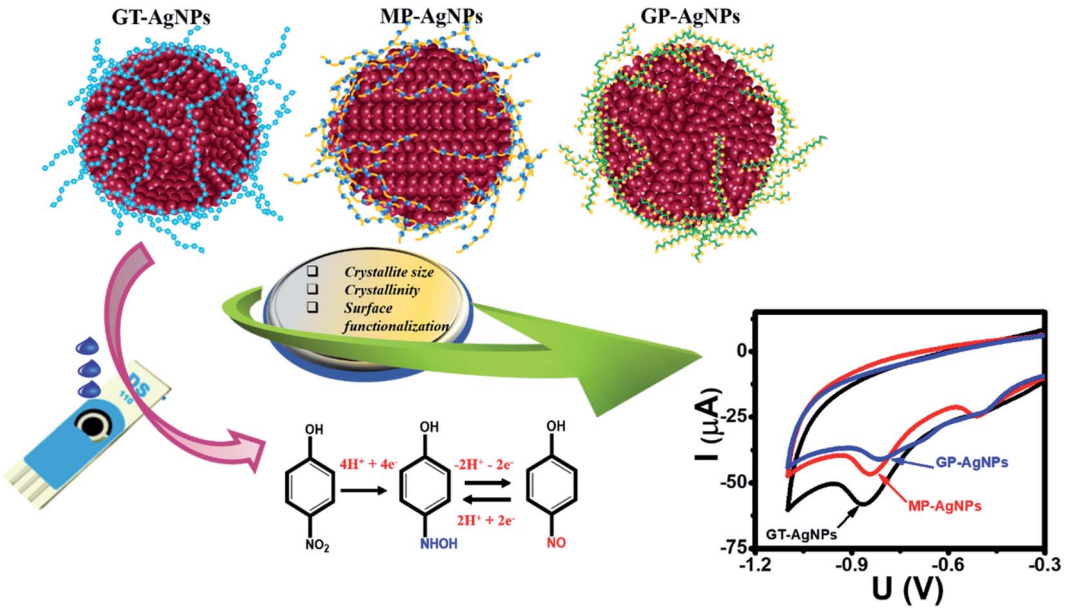

Fig. 7 Schematic illustration of the enhanced mechanism of the electrochemical sensing performance of 4-NP using SPE electrode-modified bio-AgNPs.

did not display remarkable interference in the determination of 4-NP as shown in Fig. S8.†

In order to evaluate the actual application ability of bio-AgNPs-based electrochemical sensors in a real sample, spiked tomato samples with the addition of 4-NP were utilized as model real samples. The different 4-NP concentrations of 5 μM, 10 μM, and 20 μM were spiked into tomato samples and then analyzed by DPV techniques (see Fig. S9†). The ultimate concentration of 4-NP was calculated following the regression equation of the calibration curves, as summarized in Table 2. The average recovery for GT-AgNPs/SPE was detected in the range from 48 to 97% with the relative standard deviation (RSD) within 1.9% ($n = 3$). MP-AgNPs/SPE and GP-AgNPs/SPE showed the average recoveries in the range from 73 to 123%, and the RSD values were about 2.4%. This finding suggests that the surface modification by bio-AgNPs is a crucial step in detecting 4-NP residues in real tomato samples as well as in developing the practical applicability of electrochemical sensors.

Table 2 Determination results of 4-NP residues in tomato samples using electrodes modified with GT-AgNPs/SPE, MP-AgNPs/SPE, and GP-AgNPs/SPE ($n = 3$)

Electrode	Amount added (μM)	Amount found (μM)	Recovery (%)	RSD (%)
GT-AgNPs	20	19.3	96.6	1.4
	10	7.3	73.4	1.9
	5	2.4	48.2	1.5
MP-AgNPs	20	24.8	123.8	2.4
	10	9.0	90.0	1.5
	5	3.7	73.0	1.9
GP-AgNPs	20	18.7	93.7	1.0
	10	10.4	104.0	2.4
	5	6.1	122.8	1.3

3.3. Discussion

Many studies have indicated that the improvement of the electrochemical sensing performance toward 4-NP could be achieved by using electrodes modified with nanomaterials, aiming to increase the electroactive surface area, decrease electron transfer resistance, improve electrocatalytic activity and the connection between the nanomaterials and electrode surface (Table 3). In this study, three different bio-AgNPs were synthesized from natural plant extracts, including green tea leaf, grapefruit peel, and mangosteen peel to investigate the effects of the phytochemical components and contents in each plant extract on the physicochemical parameters of the bio-AgNPs. More importantly, the differences in the size, crystallinity, and distribution ability were crucial parameters decisively affecting the conductivity, electrocatalytic activity, and adsorption efficiency of the electrodes modified with bio-AgNPs. The order of the particle size and crystallinity were GP-AgNPs > GT-AgNPs > MP-AgNPs, and GP-AgNPs < MP-AgNPs < GT-AgNPs, respectively. Accordingly, the EASA value and R_{ct} value were recorded following the order of MP-AgNPs > GP-AgNPs > GT-AgNPs, and MP-AgNPs < GP-AgNPs < GT-AgNPs. Generally, the smaller particle size is the origin of the larger electroactive surface area and is vital for enhancing electrochemical performance. Vidhu *et al.*[33] demonstrated that the AgNPs exhibited remarkable size-dependent catalytic properties in a reduction reaction of organic dyes. Another study also revealed that the catalytic activity for the reduction of 4-NP increased with the decrease in the particle size of the AgNPs.[34] The GT extract with a high content of polyphenolic compounds facilitated the formation of GT-AgNPs with smaller particle sizes, better crystallinity, and more uniform distribution. Such potential characteristics contributed to the enhanced EASA value, electron conductivity, and electrochemical response for

Table 3 Comparison of analytical parameters for the determination of 4-NP using Ag-based electrochemical sensors

Electrodes	Synthetic methods	Size of AgNPs (nm)	Technique	Linear range (μM)	LOD (μM)	Enhanced mechanism	Ref.
Bio-AgNPs/SPE	Green electrochemistry	34	DPV	0.1–25	—	Enhance the electron transfer kinetic and electrode stability *via* the bonding formation between bio-AgNPs with SPE	14
Ag-rGO/GCE	Chemical reduction	60	DPV	2–150	2	Increase electroactive surface area, electron transfer *via* the effective combination between AgNPs and rGO	35
Bio-AgNPs/GCE	Chemical	10–50	DPV	0.1–350	0.015	Increase electrocatalytic ability, electron conductivity, and compatibility of AgNPs	13
AgNWs/GCE	Chemical	70	DPV	0.6–32	0.052	Enhance electrical conductivity, catalytic activity, and interaction between the electrode surface and 4-NP	12
rGO-HNT-AgNP/SPE	Chemical	10	DPV	0.1–363.9	0.0486	Increase electroactive surface area, and electrocatalytic activity Decrease electro-transfer resistance	36
rGO-Ag/GCE	Chemical	20	AP	1–1110	0.32	Enhance electron transfer *via* strong interaction between rGO and AgNPs	37
Bio-AgNPs/GCE	Chemical	15–24	DPV	0.09–82.5	0.06	Increase surface area, catalytic capability, and high adsorptivity	38
rGO-Ag/GCE	Chemical	16	SWW	10–101	0.0012	Improve surface area, electron-transfer kinetic	9
TA@Fe_3O_4–AgNPs/GCE	Chemical	10	DPV	0.1–680.1	0.033	Improve electron transport performance and enhance 4-NP adsorption on the electrode surface	39
GT-AgNPs/SPE	Green electrochemistry	11	DPV	0.5–50	0.42	Increase electroactive surface area, electron-transfer kinetics, and electrode stability	This work
MP-AgNPs/SPE		13		1–50	0.63		
GP-AgNPs/SPE		19		5–50	0.82		

4-NP electrochemical detection, as compared with the other two bio-Ag samples. These results emphasize the important roles of the phytochemical components and contents in each plant extract on the formation of bio-AgNPs. Moreover, it stressed the synergistic effects of the size, crystallinity, and distribution of bio-AgNPs on the 4-NP electrochemical sensing performance. A comparison of the analytical parameters for the determination of 4-NP using Ag-based electrochemical sensors is given in Table 3, indicating that the bio-AgNPs-based electrochemical sensors had sufficient sensitivity and reliability for the analysis of 4-NP in food samples.

4. Conclusions

In this study, we systematically investigated and compared the electrochemical sensing performance of three electrodes modified with three types of bio-AgNPs toward 4-NP detection. According to the perspective of the structure–property–performance relationship, the obtained results indicated that the physicochemical parameters of bio-AgNPs, such as size, crystallinity, and distribution ability, were key factors in deciding the electrochemical sensing performance of 4-NP. More importantly, these characteristics could be remarkably influenced by the phytochemical components and contents in the plant extract used in the green electrochemistry synthesis process. Under optimized conditions, the GT-AgNPs-modified electrochemical sensor could determine 4-NP residue in the wide concentration range from 0.5 to 50 μM with a high sensitivity of 1.25 μA μM^{-1} cm^{-2} and a rather low LOD of 0.43 μM. The proposed sensor had good stability, satisfactory anti-interference ability, and promising detectability in real tomato samples. This finding provides insight into the influence of the plant extract components on the physicochemical parameters of bio-AgNPs synthesized, and also the roles of these physicochemical parameters in the electrochemical sensing performance in 4-NP detection.

Author contributions

N. L. N. Trang: validation, methodology, investigation, writing-original draft; D. T. N. Nga: validation, methodology, investigation; H. V. Tuan: investigation, formal analysis, writing-original draft; N. X. Dinh: conceptualization, validation, investigation, writing-review & editing; P. T. Nhung: formal analysis, writing-review & editing; L. A. Tuan: conceptualization, methodology, supervision, project administration, writing-review & editing.

Conflicts of interest

The authors declare that they have no known competing financial interests or personal relationships that could have appeared to influence the work reported in this paper.

Acknowledgements

This research was supported by the Vietnam National Foundation for Science and Technology Development (NAFOSTED) through a fundamental research project (103.02-2019.01). The authors would like to acknowledge the supports with Electrochemical, Raman, UV-vis measurements from NEB Lab at the Phenikaa University.

References

1 F. M. M. Tchieno and I. K. Tonle, p-Nitrophenol determination and remediation: an overview, *Rev. Anal. Chem.*, 2018, **37**(2), DOI: 10.1515/revac-2017-0019.

2 US Environmental Protection Agency, *4-Nitrophenol, Health and 65 Environmental Effects, Profile No. 135*, Washington, DC, 1980, vol. 1.

3 US Environmental Protection Agency, *Ambient Water Quality Criteria for Nitrophenols*, Washington, DC, 1980.

4 X. Guo, Z. Wang and S. Zhou, The separation and determination of nitrophenol isomers by high-performance capillary zone electrophoresis, *Talanta*, 2004, **64**(1), 135–139, DOI: 10.1016/j.talanta.2004.01.020.

5 W. Zhang, C. R. Wilson and N. D. Danielson, Indirect fluorescent determination of selected nitro-aromatic and pharmaceutical compounds via UV-photolysis of 2-phenylbenzimidazole-5-sulfonate, *Talanta*, 2008, **74**(5), 1400–1407.

6 M. Manera, M. Miró, J. M. Estela, V. Cerdà, M. A. Segundo and J. L. F. C. Lima, Flow-through solid-phase reflectometric method for simultaneous multiresidue determination of nitrophenol derivatives, *Anal. Chim. Acta*, 2007, **600**(1), 155–163, DOI: 10.1016/j.aca.2007.01.040.

7 J. J. Scanlon, P. A. Falquer, G. W. Robinson, G. E. O'Brien and P. E. Sturrock, High-performance liquid chromatography of nitrophenols with a swept-potential electrochemical detector, *Anal. Chim. Acta*, 1984, **158**, 169–177.

8 A. Oubina, B. Ballesteros, R. Galve, D. Barcelo and M.-P. Marco, Development and optimization of an indirect enzyme-linked immunosorbent assay for 4-nitrophenol. Application to the analysis of certified water samples, *Anal. Chim. Acta*, 1999, **387**(3), 255–266.

9 N. I. Ikhsan, P. Rameshkumar and N. M. Huang, Controlled synthesis of reduced graphene oxide supported silver nanoparticles for selective and sensitive electrochemical detection of 4-nitrophenol, *Electrochim. Acta*, 2016, **192**, 392–399, DOI: 10.1016/j.electacta.2016.02.005.

10 J. Li, D. Kuang, Y. Feng, F. Zhang, Z. Xu and M. Liu, A graphene oxide-based electrochemical sensor for sensitive determination of 4-nitrophenol, *J. Hazard. Mater.*, 2012, **201–202**, 250–259, DOI: 10.1016/j.jhazmat.2011.11.076.

11 Y. Xu, Y. Wang, Y. Ding, L. Luo, X. Liu and Y. Zhang, Determination of p-nitrophenol on carbon paste electrode modified with a nanoscaled compound oxide Mg(Ni)FeO, *J. Appl. Electrochem.*, 2013, **43**(7), 679–687, DOI: 10.1007/s10800-013-0547-0.

12 C. Zhang, S. Govindaraju, K. Giribabu, Y. S. Huh and K. Yun, AgNWs-PANI nanocomposite based electrochemical sensor for detection of 4-nitrophenol, *Sens. Actuators, B*, 2017, **252**, 616–623, DOI: 10.1016/j.snb.2017.06.039.

13 C. Karuppiah, *et al.*, Green biosynthesis of silver nanoparticles and nanomolar detection of p-nitrophenol, *J. Solid State Electrochem.*, 2014, **18**(7), 1847–1854, DOI: 10.1007/s10008-014-2425-z.

14 V. T. Hoang, *et al.*, Scalable Electrochemical Synthesis of Novel Biogenic Silver Nanoparticles and Its Application to High-Sensitive Detection of 4-Nitrophenol in Aqueous System, *Adv. Polym. Technol.*, 2021, **2021**, 1–9, DOI: 10.1155/2021/6646219.

15 I. A. Wani, Review—Recent Advances in Biogenic Silver Nanoparticles & NanoComposite Based Plasmonic-Colorimetric and Electrochemical Sensors, *ECS J. Solid State Sci. Technol.*, 2021, **10**(4), 047003, DOI: 10.1149/2162-8777/abf2df.

16 A. F. Quintero-Jaime, Á. Berenguer-Murcia, D. Cazorla-Amorós and E. Morallón, Carbon nanotubes modified with Au for electrochemical detection of prostate specific antigen: Effect of au nanoparticle size distribution, *Front. Chem.*, 2019, **7**(MAR), 1–12, DOI: 10.3389/fchem.2019.00147.

17 T. N. Pham, *et al.*, Roles of Phase Purity and Crystallinity on Chloramphenicol Sensing Performance of CuCo 2 O 4/CuFe 2 O 4 -based Electrochemical Nanosensors, *J. Electrochem. Soc.*, 2021, **168**(2), 026506, DOI: 10.1149/1945-7111/abde80.

18 N. L. N. Trang, *et al.*, Novel Eco-Friendly Synthesis of Biosilver Nanoparticles as a Colorimetric Probe for Highly Selective Detection of Fe (III) Ions in Aqueous Solution, *J. Nanomater.*, 2021, **2021**, 1–17, DOI: 10.1155/2021/5527519.

19 W. R. Rolim, *et al.*, Green tea extract mediated biogenic synthesis of silver nanoparticles: Characterization, cytotoxicity evaluation and antibacterial activity, *Appl. Surf. Sci.*, 2019, **463**, 66–74, DOI: 10.1016/j.apsusc.2018.08.203.

20 R. S. Ahmad, *et al.*, Quantitative and qualitative portrait of green tea catechins (GTC) through HPLC, *Int. J. Food Prop.*, 2014, **17**(7), 1626–1636.

21 R. Zadernowski, S. Czaplicki and M. Naczk, Phenolic acid profiles of mangosteen fruits (Garcinia mangostana), *Food Chem.*, 2009, **112**(3), 685–689, DOI: 10.1016/j.foodchem.2008.06.030.

22 A. Fejzić and S. Ćavar, Phenolic compounds and antioxidant activity of some citruses, *Bull. Chem. Technol. Bosnia Herzegovina*, 2014, **42**, 1–4.

23 G. M. Carmen, L. R. José, L. G. Pilar, B. Amparo and G. Antonio, Volatile compounds in citrus essential oils: a comprehensive review, *Front. Plant Sci.*, 2019, **10**, 12, DOI: 10.3389/fpls.2019.00012.

24 R. D. Rivera-Rangel, M. P. González-Muñoz, M. Avila-Rodriguez, T. A. Razo-Lazcano and C. Solans, Green synthesis of silver nanoparticles in oil-in-water microemulsion and nano-emulsion using geranium leaf aqueous extract as a reducing agent, *Colloids Surf., A*, 2018, **536**(July 2017), 60–67, DOI: 10.1016/j.colsurfa.2017.07.051.

25 B. Banumathi, *et al.*, Toxicity of Camellia sinensis-Fabricated Silver Nanoparticles on Invertebrate and Vertebrate Organisms: Morphological Abnormalities and DNA Damages, *J. Cluster Sci.*, 2017, **28**(4), 2027–2040, DOI: 10.1007/s10876-017-1201-5.

26 L. O. Cinteza, *et al.*, Chitosan-stabilized ag nanoparticles with superior biocompatibility and their synergistic antibacterial effect in mixtures with essential oils, *Nanomaterials*, 2018, **8**(10), 826, DOI: 10.3390/nano8100826.

27 D. Kumar, G. Kumar and V. Agrawal, Green synthesis of silver nanoparticles using Holarrhena antidysenterica (L.) Wall.bark extract and their larvicidal activity against dengue and filariasis vectors, *Parasitol. Res.*, 2018, **117**(2), 377–389, DOI: 10.1007/s00436-017-5711-8.

28 J. B. Raoof, F. Chekin, R. Ojani, S. Barari, M. Anbia and S. Mandegarzad, Synthesis and characterization of ordered mesoporous carbon as electrocatalyst for simultaneous determination of epinephrine and acetaminophen, *J. Solid State Electrochem.*, 2012, **16**(12), 3753–3760, DOI: 10.1007/s10008-012-1807-3.

29 W.-C. Wu, H.-W. Chang and Y.-C. Tsai, Electrocatalytic detection of dopamine in the presence of ascorbic acid and uric acid at silicon carbide coated electrodes, *Chem. Commun.*, 2011, **47**(22), 6458, DOI: 10.1039/c1cc11162k.

30 B. Dinesh and R. Saraswathi, Electrochemical synthesis of nanostructured copper-curcumin complex and its electrocatalytic application towards reduction of 4-nitrophenol, *Sens. Actuators, B*, 2017, **253**(June), 502–512, DOI: 10.1016/j.snb.2017.06.149.

31 N. X. Dinh, *et al.*, Ultrasensitive determination of chloramphenicol in pork and chicken meat samples using a portable electrochemical sensor: effects of 2D nanomaterials on the sensing performance and stability, *New J. Chem.*, 2021, **45**, 7622–7636, DOI: 10.1039/d1nj00582k.

32 J. N. Baby, B. Sriram, S. F. Wang and M. George, Effect of Various Deep Eutectic Solvents on the Sustainable Synthesis of MgFe2O4 Nanoparticles for Simultaneous Electrochemical Determination of Nitrofurantoin and 4-Nitrophenol, *ACS Sustainable Chem. Eng.*, 2020, **8**(3), 1479–1486, DOI: 10.1021/acssuschemeng.9b05755.

33 V. K. Vidhu and D. Philip, Catalytic degradation of organic dyes using biosynthesized silver nanoparticles, *Micron*, 2014, **56**, 54–62, DOI: 10.1016/j.micron.2013.10.006.

34 D. Badma Priya and I. V. Asharani, Size Dependent Catalytic Activity of Actinodaphne madraspatana Bedd Leaves Mediated Silver Nanoparticles, *J. Cluster Sci.*, 2017, **28**(4), 1837–1856, DOI: 10.1007/s10876-017-1185-1.

35 N. Ahmad, A. S. Al-Fatesh, R. Wahab, M. Alam and A. H. Fakeeha, Synthesis of silver nanoparticles decorated on reduced graphene oxide nanosheets and their electrochemical sensing towards hazardous 4-nitrophenol, *J. Mater. Sci.: Mater. Electron.*, 2020, **31**(14), 11927–11937, DOI: 10.1007/s10854-020-03747-3.

36 K. Y. Hwa, T. S. K. Sharma and A. Ganguly, Design strategy of rGO-HNT-AgNPs based hybrid nanocomposite with enhanced performance for electrochemical detection of 4-nitrophenol, *Inorg. Chem. Front.*, 2020, **7**(10), 1981–1994, DOI: 10.1039/d0qi00006j.

37 A. M. Noor, P. Rameshkumar, N. Yusoff, H. N. Ming and M. S. Sajab, Microwave synthesis of reduced graphene oxide decorated with silver nanoparticles for electrochemical determination of 4-nitrophenol, *Ceram. Int.*, 2016, **42**(16), 18813–18820, DOI: 10.1016/j.ceramint.2016.09.026.

38 R. Karthik, Y. S. Hou, S. M. Chen, A. Elangovan, M. Ganesan and P. Muthukrishnan, Eco-friendly synthesis of Ag-NPs using Cerasus serrulata plant extract - Its catalytic, electrochemical reduction of 4-NPh and antibacterial activity, *J. Ind. Eng. Chem.*, 2016, **37**(April), 330–339, DOI: 10.1016/j.jiec.2016.03.044.

39 A. Sangili, M. Annalakshmi, S. M. Chen, P. Balasubramanian and M. Sundrarajan, Synthesis of silver nanoparticles decorated on core-shell structured tannic acid-coated iron oxide nanospheres for excellent electrochemical detection and efficient catalytic reduction of hazardous 4-nitrophenol, *Composites, Part B*, 2019, **162**, 33–42, DOI: 10.1016/j.compositesb.2018.10.084.